

Probing CP violation in $\gamma\gamma\rightarrow W^+W^-$ with polarized photon beams

S. Y. Choi and K. Hagiwara
Theory Group, KEK, Tsukuba, Ibaraki 305, Japan

M. S. Baek
Department of Physics and Center for Theoretical Physics, Seoul National University, Seoul 151-742, Korea
 (Received 22 May 1996)

We demonstrate in a general framework that polarized photons by backscattered laser beams of adjustable frequencies at a TeV linear e^+e^- collider provide us with a very efficient mechanism to probe CP violation in two-photon collisions. CP violation in the process $\gamma\gamma\rightarrow W^+W^-$ is investigated in detail with linearly polarized photon beams. There are two useful CP -odd asymmetries that do not require detailed information on W decay products. The sensitivity to the CP -odd form factors are studied quantitatively by assuming a perfect $e-\gamma$ conversion and the $20\text{ fb}^{-1} e^+e^-$ integrated luminosity at the e^+e^- c.m. energies $\sqrt{s}=0.5$ and 1.0 TeV. The sensitivity is so high that such experiments will allow us to probe new CP violation effects beyond the limits from some specific models with reasonable physics assumptions. We find that a counting experiment of W^+W^- events in the two-photon mode with adjustable laser frequencies can have much stronger sensitivity to the CP -odd $\gamma(\gamma)WW$ form factors than can a W^+W^- decay-correlation experiment with a perfect detector achieve in the e^+e^- mode. [S0556-2821(96)05121-1]

PACS number(s): 14.70.Bh, 13.88.+e, 14.70.Hp

I. INTRODUCTION

Even though the standard model (SM) has been successful in explaining all the experimental data up to date, it is believed that the SM is merely an effective theory valid at and below the weak scale and that new physics beyond the SM should appear at higher energies. We may expect to find new physics beyond the SM at high precision experiments on quantities, whose SM values are suppressed. An interesting class of quantities, where the SM contributions are strongly suppressed, are those with CP violation. In the SM, CP violation stems from the complex phase of the Kobayashi-Maskawa (KM) quark-mixing matrix [1] and the size of CP violation is often extremely small. In contrast, various new physics scenarios on CP violation lead to comparatively large CP violation [2]. Any observable CP -odd violations should, hence, be a good direct means to look for new physics effects.

The next generation of e^+e^- colliders [3] will offer interesting possibilities for studying physics of the heavy H , t -quark, and the W bosons either in the e^+e^- mode or in the $\gamma\gamma$ mode. Linear collider physics in the e^+e^- mode has been studied intensively for the past decade. Recently, it has become clear that the $\gamma\gamma$ mode (as well as the $e\gamma$ mode) [4] can provide a good complement to experiments in the e^+e^- mode. For instance, it has been shown that the $\gamma\gamma$ mode has a unique advantage in the determination of the Higgs-two-photon coupling [5] and its CP properties [6]. Pair production of the top-quark [7] and the W boson [8,9] in the $\gamma\gamma$ mode also has been studied as probes of CP violation in physics beyond the SM. Most works [7,8] have concentrated on the use of the spin correlations of the pair-produced top-quarks and the W bosons, which require detailed study of their decay products. Recently, it has been pointed out [10] that the (linearly) polarized photon beams can provide us with very powerful tests of the top-quark electric dipole mo-

ment (EDM) without any information on the $t\bar{t}$ decay patterns. Use of the $\gamma\gamma$ mode with linearly polarized photon beams for studying CP violations in the process $\gamma\gamma\rightarrow W^+W^-$ also has been considered by Bélanger and Couture [9].

In the present work, we demonstrate in a rather general framework that polarized photons by backscattered laser beams of adjustable frequencies provide us with a very efficient mechanism to probe CP violation in the two-photon mode. We then give an extensive investigation of the possibility of probing CP violation with (linearly) polarized photon beams in the process $\gamma\gamma\rightarrow W^+W^-$. We extend in a systematic way the previous work [9] so as to cover an arbitrary angle between polarization directions of two photon beams and an arbitrary laser beam frequency. We find, in particular, that adjusting the laser beam frequency is essential to optimizing the sensitivity to CP violation phenomena. Furthermore, we study effects of all the possible dimension-six CP -odd operators composed of the Higgs doublet and the electroweak gauge bosons.

The W^+W^- production in the $\gamma\gamma$ mode has several unique features in contrast to that in the e^+e^- mode, $e^+e^-\rightarrow W^+W^-$. In the e^+e^- mode, a pair of W 's are produced via an annihilation of the colliding e^- and e^+ , where the electronic chirality should be preserved along the electron line [11] due to the very small electron mass in the SM. This forces the positron helicity to be opposite to the electron helicity such that the initial e^+e^- configuration is always CP even. On the contrary, there exists no apparent helicity selection mechanism in the $\gamma\gamma$ production of W^+W^- . This feature makes any CP -odd $\gamma\gamma$ configuration in the initial state a good probe of CP violation in the two-photon mode.

The process $\gamma\gamma\rightarrow W^+W^-$, which is characterized by the angle between the W^+ momentum and the γ momentum in the c.m. frame, and the helicities of the particles, is C , P , and

CP self-conjugate, when the particle helicities are averaged over. For this reason, the helicities (but not all of them) need to be determined or analyzed statistically to observe violations of these discrete symmetries. One can take two approaches in analyzing the process $\gamma\gamma \rightarrow W^+W^-$. One approach makes use of the spin correlations of the two decaying W bosons that can be measured by studying correlations in the W^+W^- decay-product system, $(q\bar{q}')(l\bar{\nu})$ or $(\bar{l}\nu)(l\bar{\nu})$. The other method is to employ polarized photon beams to measure various polarization asymmetries of the initial states. Note that in the e^+e^- mode, only the former method, the spin correlations of final decay products, is available. The two-photon mode allows us to combine the two methods. The use of the former technique in the two-photon collisions is essentially the same as that in e^+e^- collisions [12–14] with one crucial difference; in e^+e^- collisions the spin of the W^+W^- system is restricted to $J \geq 1$, while in $\gamma\gamma$ collisions, $J=0$ is allowed. For a specific final state such as W^+W^- and $t\bar{t}$, the two-photon cross section is larger than the corresponding e^+e^- cross section. Especially, the W pair cross section in the two-photon mode is much larger than that in the e^+e^- mode because the $\gamma\gamma$ mode has contributions from the $J=0$ channel near threshold and a t -channel W boson exchange. Moreover, it is easy to produce (linearly) polarized photon beams through the Compton backscattering of polarized laser-light off the initial electron or positron beams. Hence, the $\gamma\gamma$ mode of future linear colliders provides some unique opportunities to probe CP violation.

In Sec. II we describe in a general framework how the photon polarization in the two-photon mode can be employed to study CP and CPT invariances. Here \bar{T} is the so-called naive-time-reversal operation which reverses the signs of the three momenta and spin of all particles, but does not reverse the direction of the flow of time. The notation is introduced in Ref. [12]. Assuming that two-photon beams are purely linearly polarized in the colliding $\gamma\gamma$ c.m. frame, we construct two CP -odd and CPT -even asymmetries which allow us to probe CP violation without any direct information on the momenta and polarization of the final-state particles. All that we have to do is to count the number of signal events for a specific polarization configuration of the initial two photons. In Sec. III we give a short review of a mechanism of producing highly energetic photons, the Compton backscattering of laser photons off the electron or positron beam [15], and we introduce two functions that measure the partial transfers of the linear polarization from the laser beams to the Compton backscattered photon beams. We then investigate in detail which parameters are crucial to optimize the observation of CP violation with linearly polarized laser beams.

In Sec. IV we study consequences of CP -violating new interactions in the bosonic sector of the SM, by adopting a model-independent approach, where we allow all six dimension-six operators of the electroweak gauge bosons and the Higgs doublet that are CP odd [16]. We identify all the vertices and present the Feynman rules relevant for the process $\gamma\gamma \rightarrow W^+W^-$. In Sec. V, including all the new contributions, we present the helicity amplitudes of the $\gamma\gamma \rightarrow W^+W^-$ reaction. Folding with the effective two-

photon energy spectrum, we then estimate the size of the two CP -odd asymmetries for a set of CP -odd operator coefficients. In Sec. VI we present the $1\text{-}\sigma$ sensitivities to the CP -odd parameters by assuming a perfect $e\text{-}\gamma$ conversion in the Compton backscattering mechanism for an e^+e^- integrated luminosity of 20 fb^{-1} . We then compare the sensitivities in the two-photon mode with those in the e^+e^- mode under the same luminosity and c.m. energy, by restricting ourselves to the W EDM and the W magnetic quadrupole moment (MQD). Finally, in Sec. VII we summarize our findings and give conclusions.

II. PHOTON POLARIZATION

In this section we fix our notation to describe in a general framework how photon polarization can provide us with an efficient mechanism to probe CP and CPT invariances in the two-photon mode. With purely linearly polarized photon beams, we classify all the distributions according to their CP and CPT properties. Then, we show explicitly how linearly polarized photon beams allow us to construct two CP -odd and CPT -even asymmetries, which do not require detailed information on the momenta and polarization of the final-state particles.

A. Formalism

A photon should be polarized transversely. For the photon momentum in the positive z direction, the helicity- ± 1 polarization vectors are given by

$$|\pm\rangle = \mp \frac{1}{\sqrt{2}}(0, 1, \pm i, 0). \quad (2.1)$$

Generally, a purely polarized photon beam state is a linear combination of two helicity states and the photon polarization vector can be expressed in terms of two angles α and ϕ in a given coordinate system as

$$|\alpha, \phi\rangle = -\cos(\alpha)e^{-i\phi}|+\rangle + \sin(\alpha)e^{i\phi}|-\rangle, \quad (2.2)$$

where $0 \leq \alpha \leq \pi/2$ and $0 \leq \phi \leq 2\pi$. Then, the 2×2 photon density matrix ρ [15,17] in the helicity basis $\{|+\rangle, |-\rangle\}$ is given by

$$\rho \equiv |\alpha, \phi\rangle\langle\alpha, \phi| = \frac{1}{2} \begin{pmatrix} 1 + \cos(2\alpha) & -\sin(2\alpha)e^{2i\phi} \\ -\sin(2\alpha)e^{-2i\phi} & 1 - \cos(2\alpha) \end{pmatrix}. \quad (2.3)$$

It is easy to read from Eq. (2.3) that the degrees of circular and linear polarization are, respectively,

$$\xi = \cos(2\alpha), \quad \eta = \sin(2\alpha), \quad (2.4)$$

and the direction of maximal linear polarization is denoted by the azimuthal angle ϕ in the given coordinate system. Note that $\xi^2 + \eta^2 = 1$ as expected for a purely polarized photon. For a partially polarized photon beam, it is necessary to rescale ξ and η by its degree of polarization P ($0 \leq P \leq 1$) as

$$\xi = P\cos(2\alpha), \quad \eta = P\sin(2\alpha), \quad (2.5)$$

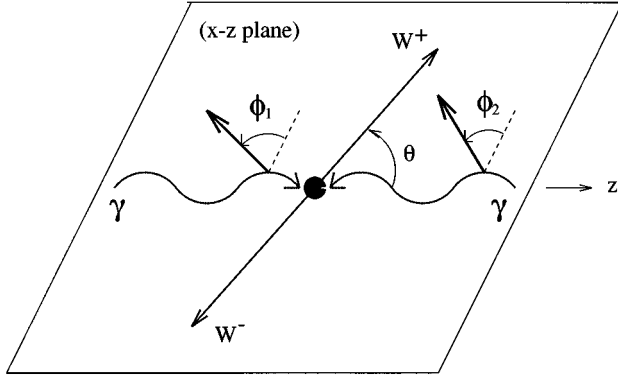


FIG. 1. The coordinate system in the colliding $\gamma\gamma$ c.m. frame. The scattering angle θ and the azimuthal angles ϕ_1 and ϕ_2 for the linear polarization directions measured from the scattering plane are given.

such that $\xi^2 + \eta^2 = P^2$.

Let us now consider the two-photon system in the center-of-mass frame, where one photon momentum is along the positive z direction. The state vector of the two photons is

$$\begin{aligned}
 |\alpha_1, \phi_1; \alpha_2, \phi_2\rangle &= |\alpha_1, \phi_1\rangle |\alpha_2, -\phi_2\rangle \\
 &= \cos(\alpha_1)\cos(\alpha_2)e^{-i(\phi_1-\phi_2)}|++\rangle \\
 &\quad - \cos(\alpha_1)\sin(\alpha_2)e^{-i(\phi_1+\phi_2)}|+-\rangle \\
 &\quad - \sin(\alpha_1)\cos(\alpha_2)e^{i(\phi_1+\phi_2)}|-+\rangle \\
 &\quad + \sin(\alpha_1)\sin(\alpha_2)e^{i(\phi_1-\phi_2)}|--\rangle,
 \end{aligned} \tag{2.6}$$

and then the transition amplitude from the polarized two-photon state to a final state X in the two-photon c.m. frame is simply given by

$$\langle X|M|\alpha_1, \phi_1; \alpha_2, \phi_2\rangle. \tag{2.7}$$

The azimuthal angles ϕ_1 and ϕ_2 are the directions of maximal linear polarization of the two photons, respectively, in a common coordinate system (see Fig. 1). In the process $\gamma\gamma \rightarrow W^+W^-$, the scattering plane is taken to be the x - z plane in the actual calculation of the helicity amplitudes. The maximal linear polarization angles are then chosen as follows. The angle ϕ_1 (ϕ_2) is the azimuthal angle of the maximal linear polarization of the photon beam, whose momentum is in the positive (negative) z direction, with respect to the direction of the W^+ momentum. Note that we have used $|\alpha_2, -\phi_2\rangle$ in Eq. (2.6) for the photon whose momentum is along the negative z direction in order to employ a common coordinate system for the two-photon system.

For later convenience, we introduce the abbreviation

$$M_{\lambda_1\lambda_2} = \langle X|M|\lambda_1\lambda_2\rangle, \tag{2.8}$$

and two angular variables:

$$\chi = \phi_1 - \phi_2, \quad \phi = \phi_1 + \phi_2, \tag{2.9}$$

where $-2\pi \leq \chi \leq 2\pi$ and $0 \leq \phi \leq 4\pi$ for a fixed χ . It should be noted that (i) the azimuthal angle difference χ is independent of the final state, while the azimuthal angle sum ϕ depends on the scattering plane, and (ii) both angles are invariant with respect to the Lorentz boost along the two-photon beam direction.

It is now straightforward to obtain the angular dependence of the $\gamma\gamma \rightarrow X$ cross section on the initial beam polarizations

$$\begin{aligned}
 \Sigma(\xi, \bar{\xi}; \eta, \bar{\eta}; \chi, \phi) &\equiv \sum_X |\langle X|M|\xi, \bar{\xi}; \eta, \bar{\eta}; \chi, \phi\rangle|^2 = \frac{1}{4} \sum_X (|M_{++}|^2 + |M_{+-}|^2 + |M_{-+}|^2 + |M_{--}|^2) \\
 &\quad + \frac{\xi}{4} \sum_X (|M_{++}|^2 + |M_{+-}|^2 - |M_{-+}|^2 - |M_{--}|^2) + \frac{\bar{\xi}}{4} \sum_X (|M_{++}|^2 - |M_{+-}|^2 + |M_{-+}|^2 - |M_{--}|^2) \\
 &\quad + \frac{\xi\bar{\xi}}{4} \sum_X (|M_{++}|^2 - |M_{+-}|^2 - |M_{-+}|^2 + |M_{--}|^2) - \frac{\eta}{2} \text{Re} \left[e^{-i(\chi+\phi)} \sum_X (M_{++}M_{-+}^* + M_{+-}M_{--}^*) \right] \\
 &\quad - \frac{\bar{\eta}}{2} \text{Re} \left[e^{-i(\chi-\phi)} \sum_X (M_{++}M_{+-}^* + M_{-+}M_{--}^*) \right] - \frac{\eta\bar{\xi}}{2} \text{Re} \left[e^{-i(\chi+\phi)} \sum_X (M_{++}M_{-+}^* - M_{+-}M_{--}^*) \right] \\
 &\quad - \frac{\bar{\eta}\xi}{2} \text{Re} \left[e^{-i(\chi-\phi)} \sum_X (M_{++}M_{+-}^* - M_{-+}M_{--}^*) \right] + \frac{\eta\bar{\eta}}{2} \text{Re} \left[e^{-2i\phi} \sum_X (M_{+-}M_{-+}^*) + e^{-2i\chi} \right. \\
 &\quad \left. \times \sum_X (M_{++}M_{--}^*) \right],
 \end{aligned} \tag{2.10}$$

where the summation over X is for the polarizations of the final states, and $(\xi, \bar{\xi})$ denote the degrees of circular polarization and $(\eta, \bar{\eta})$ denote those of linear polarization of the two initial photon beams, respectively. They are expressed in terms of two parameters α_1 and α_2 by

$$\begin{aligned}
 \xi &= P \cos(2\alpha_1), & \bar{\xi} &= \bar{P} \cos(2\alpha_2), \\
 \eta &= P \sin(2\alpha_1), & \bar{\eta} &= \bar{P} \sin(2\alpha_2),
 \end{aligned} \tag{2.11}$$

where P and \bar{P} ($0 \leq P, \bar{P} \leq 1$) are the polarization degrees of the two colliding photons.

It is easy to check that there are sixteen independent terms, which are all measurable in polarized two-photon collisions. We find that purely linearly polarized photon beams allow us to determine nine terms among all the sixteen terms, while purely circularly polarized photon beams allow us to determine only four terms. The first term in Eq. (2.10), which corresponds to the unpolarized cross section, is determined in both cases. However, both circular and linear polarizations are needed to determine the remaining four terms.

Even though we obtain more information with both circularly and linearly polarized beams, we study in this paper mainly the case, where two photons are linearly polarized, but not circularly polarized. The expression of the angular dependence then simplifies greatly to

$$D(\eta, \bar{\eta}; \chi, \phi) = \Sigma_{\text{unpol}} - \frac{1}{2} \text{Re}[(\eta e^{-i\phi} + \bar{\eta} e^{i\phi}) e^{-i\chi} \Sigma_{02}] + \frac{1}{2} \text{Re}[(\eta e^{-i\phi} - \bar{\eta} e^{i\phi}) e^{-i\chi} \Delta_{02}] + \eta \bar{\eta} \text{Re}[e^{-2i\phi} \Sigma_{22} + e^{-2i\chi} \Sigma_{00}], \quad (2.12a)$$

$$\begin{aligned} &= \Sigma_{\text{unpol}} - \frac{1}{2} [\eta \cos(\phi + \chi) + \bar{\eta} \cos(\phi - \chi)] \mathcal{R}(\Sigma_{02}) + \frac{1}{2} [\eta \sin(\phi + \chi) - \bar{\eta} \sin(\phi - \chi)] \mathcal{I}(\Sigma_{02}) - \frac{1}{2} [\eta \cos(\phi + \chi) \\ &\quad - \bar{\eta} \cos(\phi - \chi)] \mathcal{R}(\Delta_{02}) + \frac{1}{2} [\eta \sin(\phi + \chi) + \bar{\eta} \sin(\phi - \chi)] \mathcal{I}(\Delta_{02}) + \eta \bar{\eta} \cos(2\phi) \mathcal{R}(\Sigma_{22}) + \eta \bar{\eta} \sin(2\phi) \mathcal{I}(\Sigma_{22}) \\ &\quad + \eta \bar{\eta} \cos(2\chi) \mathcal{R}(\Sigma_{00}) + \eta \bar{\eta} \sin(2\chi) \mathcal{I}(\Sigma_{00}), \end{aligned} \quad (2.12b)$$

where \mathcal{R} and \mathcal{I} are for real and imaginary parts, respectively, and the invariant functions are defined as

$$\begin{aligned} \Sigma_{\text{unpol}} &= \frac{1}{4} \sum_X (|M_{++}|^2 + |M_{+-}|^2 + |M_{-+}|^2 + |M_{--}|^2), \\ \Sigma_{02} &= \frac{1}{2} \sum_X [M_{++}(M_{+-}^* + M_{-+}^*) + (M_{+-} + M_{-+})M_{--}^*], \\ \Delta_{02} &= \frac{1}{2} \sum_X [M_{++}(M_{+-}^* - M_{-+}^*) - (M_{+-} - M_{-+})M_{--}^*], \\ \Sigma_{22} &= \frac{1}{2} \sum_X (M_{+-}M_{-+}^*), \quad \Sigma_{00} = \frac{1}{2} \sum_X (M_{++}M_{--}^*), \end{aligned} \quad (2.13)$$

with the subscripts 0 and 2 representing the magnitude of the sum of the helicities of the initial two-photon system.

B. Symmetry properties

It is useful to classify the invariant functions according to their transformation properties under the discrete symmetries, CP and CPT [12]. We find that CP invariance leads to the relations

$$\sum_X (M_{\lambda_1 \lambda_2} M_{\lambda'_1 \lambda'_2}^*) = \sum_X (M_{-\lambda_2, -\lambda_1} M_{-\lambda'_2, -\lambda'_1}^*), \quad (2.14a)$$

$$d\sigma(\phi, \chi; \eta, \bar{\eta}) = d\sigma(\phi, -\chi; \bar{\eta}, \eta), \quad (2.14b)$$

and, if there are no absorptive parts in the amplitudes, CPT invariance leads to the relations

$$\sum_X (M_{\lambda_1 \lambda_2} M_{\lambda'_1 \lambda'_2}^*) = \sum_X (M_{-\lambda_2, -\lambda_1}^* M_{-\lambda'_2, -\lambda'_1}), \quad (2.15a)$$

$$d\sigma(\phi, \chi; \eta, \bar{\eta}) = d\sigma(-\phi, \chi; \bar{\eta}, \eta). \quad (2.15b)$$

The nine invariant functions in Eq. (2.12b) then can be divided into four categories under CP and CPT : even-even, even-odd, odd-even, and odd-odd terms as in Table I. CP -odd coefficients measure directly CP violation and CPT -odd terms indicate rescattering effects (absorptive parts in the scattering amplitudes). Table I shows that there exist three CP -odd functions; $\mathcal{I}(\Sigma_{02})$, $\mathcal{I}(\Sigma_{00})$, and $\mathcal{R}(\Delta_{02})$. Here, \mathcal{R} and \mathcal{I} are for real and imaginary parts, respectively. While the first two terms are CPT even, the last term $\mathcal{R}(\Delta_{02})$ is CPT odd. Since the CPT -odd term $\mathcal{R}(\Delta_{02})$ requires the absorptive part in the amplitude, it is generally expected to be smaller in magnitude than the CPT -even terms. We, therefore, study the two CP -odd and CPT -even distributions, $\mathcal{I}(\Sigma_{02})$ and $\mathcal{I}(\Sigma_{00})$ [18].

We can define two CP -odd asymmetries from the two distributions, $\mathcal{I}(\Sigma_{02})$ and $\mathcal{I}(\Sigma_{00})$. First, we note that the Σ_{00} term does not depend on the azimuthal angle ϕ , whereas the Σ_{02} does. In order to improve the observability, we may integrate the $\mathcal{I}(\Sigma_{02})$ term over the azimuthal angle ϕ with an appropriate weight function. Without any loss of generality, we can take $\eta = \bar{\eta}$. Then, the quantity $\mathcal{I}(\Sigma_{00})$ in Eq. (2.12b) can be separated by taking the difference of the distributions at $\chi = \pm \pi/4$ and the $\mathcal{I}(\Sigma_{02})$ by taking the difference of the distributions at $\chi = \pm \pi/2$. As a result, we obtain two integrated CP -odd asymmetries,

TABLE I. CP and CPT properties of the invariant functions and the angular distributions.

CP	CPT	Invariant functions	Angular dependences
even	even	Σ_{unpol} $\mathcal{R}(\Sigma_{02})$ $\mathcal{R}(\Sigma_{22})$ $\mathcal{R}(\Sigma_{00})$	$\eta \cos(\phi + \chi) + \bar{\eta} \cos(\phi - \chi)$ $\eta \bar{\eta} \cos(2\phi)$ $\eta \bar{\eta} \cos(2\chi)$
even	odd	$\mathcal{I}(\Delta_{02})$ $\mathcal{I}(\Sigma_{22})$	$\eta \sin(\phi + \chi) + \bar{\eta} \sin(\phi - \chi)$ $\eta \bar{\eta} \sin(2\phi)$
odd	even	$\mathcal{I}(\Sigma_{02})$ $\mathcal{I}(\Sigma_{00})$	$\eta \sin(\phi + \chi) - \bar{\eta} \sin(\phi - \chi)$ $\eta \bar{\eta} \sin(2\chi)$
odd	odd	$\mathcal{R}(\Delta_{02})$	$\eta \cos(\phi + \chi) - \bar{\eta} \cos(\phi - \chi)$

$$\hat{A}_{02} = \left(\frac{2}{\pi} \right) \frac{\mathcal{I}(\Sigma_{02})}{\Sigma_{\text{unpol}}}, \quad \hat{A}_{00} = \frac{\mathcal{I}(\Sigma_{00})}{\Sigma_{\text{unpol}}}, \quad (2.16)$$

where the factor $(2/\pi)$ in the \hat{A}_{02} stems from taking the average over the azimuthal angle ϕ with the weight function $\text{sgn}(\cos\phi)$:

$$\hat{A}_{02} = \frac{\int_0^{4\pi} d\phi [\text{sgn}(\cos\phi)] \left[\left(\frac{d\sigma}{d\phi} \right)_{\chi=\pi/2} - \left(\frac{d\sigma}{d\phi} \right)_{\chi=-\pi/2} \right]}{\int_0^{4\pi} d\phi \left[\left(\frac{d\sigma}{d\phi} \right)_{\chi=\pi/2} + \left(\frac{d\sigma}{d\phi} \right)_{\chi=-\pi/2} \right]}, \quad (2.17a)$$

$$\hat{A}_{00} = \frac{\int_0^{4\pi} d\phi \left[\left(\frac{d\sigma}{d\phi} \right)_{\chi=\pi/4} - \left(\frac{d\sigma}{d\phi} \right)_{\chi=-\pi/4} \right]}{\int_0^{4\pi} d\phi \left[\left(\frac{d\sigma}{d\phi} \right)_{\chi=\pi/4} + \left(\frac{d\sigma}{d\phi} \right)_{\chi=-\pi/4} \right]}. \quad (2.17b)$$

In pair production processes such as $\gamma\gamma \rightarrow W^+W^-$, all the distributions, Σ_i , can be integrated over the scattering angle θ with a CP -even angular cut so as to test CP violation.

III. PHOTON LINEAR COLLIDER

In this section we give a short review of the powerful mechanism of providing an energetic, highly polarized photon beam; the Compton laser backscattering [15] off energetic electron or positron beams. After the review, we introduce two functions to describe partial linear polarization transfer from the laser beams to the backscattered photon beams for the photon-photon collisions.

We assume that the electron or positron beams are unpolarized and the laser beams are purely linearly polarized. Even in that case, the backscattered photon beam is not purely linearly polarized, but only part of the laser linear polarization is transferred to the backscattered energetic high-energy photon beam.

A. Photon spectrum

We consider the situation where a purely linearly polarized laser beam of frequency ω_0 is focused upon an unpolarized electron or positron beam of energy E . In the collision of a laser photon beam and a linear electron beam, a high energy photon beam of energy ω , which is partially linearly polarized, is emitted at a very small angle, along with the scattered electron beam of energy $E' = E - \omega$. The kinematics of the Compton backscattering process is then characterized by the dimensionless parameters x and y :

$$x = \frac{4E\omega_0}{m_e^2} \approx 15.3 \left(\frac{E}{\text{TeV}} \right) \left(\frac{\omega_0}{\text{eV}} \right), \quad y = \frac{\omega}{E}. \quad (3.1)$$

In general, the backscattered photon energies increase with x ; the maximum photon energy fraction is given by $y_m = x/(1+x)$. Operation below the threshold [15] for e^+e^- pair production in collisions between the laser beam and the Compton-backscattered photon beam requires

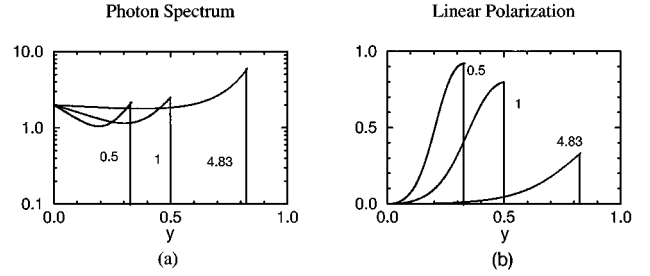


FIG. 2. (a) The photon energy spectrum and (b) the degree of linear polarization of the Compton backscattered photon beam for $x = 4E\omega_0/m_e^2 = 0.5, 1, \text{ and } 4.83$.

$x \leq 2(1 + \sqrt{2}) \approx 4.83$; the lower bound on x depends on the lowest available laser frequency and the production threshold of a given final state.

The backscattered photon energy spectrum is given by the function

$$\phi_0(y) = \frac{1}{1-y} + 1 - y - 4r(1-r), \quad (3.2)$$

where $r = y/[x(1-y)]$. Figure 2(a) shows the photon energy spectrum for various values of x . Clearly, large values of x are favored to produce highly energetic photons. On the other hand, the degree of linear polarization of the backscattered photon beam is given by [15]

$$\eta(y) = \frac{2r^2}{\phi_0(y)}. \quad (3.3)$$

The maximum linear polarization is reached for $y = y_m$ [see Fig. 2(b)],

$$\eta_{\text{max}} = \eta(y_m) = \frac{2(1+x)}{1+(1+x)^2}, \quad (3.4)$$

and approaches unity for small values of x . In order to retain large linear polarization, we should keep the x value as small as possible.

B. Linear polarization transfers

In the two-photon collision case, only part of each laser linear polarization is transferred to the high-energy photon beam. We introduce two functions, \mathcal{A}_η and $\mathcal{A}_{\eta\eta}$, to denote the degrees of linear polarization transfer [19] as

$$\mathcal{A}_\eta(\tau) = \frac{\langle \phi_0 \phi_3 \rangle_\tau}{\langle \phi_0 \phi_0 \rangle_\tau}, \quad \mathcal{A}_{\eta\eta}(\tau) = \frac{\langle \phi_3 \phi_3 \rangle_\tau}{\langle \phi_0 \phi_0 \rangle_\tau}, \quad (3.5)$$

where $\phi_3(y) = 2r^2$ and τ is the ratio of the $\gamma\gamma$ c.m. energy squared \hat{s} to the e^+e^- collider energy squared s . The function \mathcal{A}_η is for the collision of an unpolarized photon beam and a linearly polarized photon beam and the function $\mathcal{A}_{\eta\eta}$ is for the collision of two linearly polarized photon beams. The convolution integrals $\langle \phi_i \phi_j \rangle_\tau$ ($i, j = 0, 3$) for a fixed value of τ are defined as

$$\langle \phi_i \phi_j \rangle_\tau = \frac{1}{\mathcal{N}^2(x)} \int_{\tau/y_m}^{y_m} \frac{dy}{y} \phi_i(y) \phi_j(\tau/y), \quad (3.6)$$

where the normalization factor $\mathcal{N}(x)$ is given by the integral of the photon energy spectrum ϕ_0 over y as

$$\begin{aligned} \mathcal{N}(x) &= \int_0^{y_m} \phi_0(y) dy \\ &= \ln(1+x) \left[1 - \frac{4}{x} - \frac{8}{x^2} \right] + \frac{1}{2} + \frac{8}{x} - \frac{1}{2(1+x)^2}. \end{aligned} \quad (3.7)$$

The event rates of the $\gamma\gamma \rightarrow X$ reaction with polarized photons can be obtained by folding a photon luminosity spectral function with the $\gamma\gamma \rightarrow X$ production cross section as (for $\eta = \bar{\eta}$)

$$dN_{\gamma\gamma \rightarrow X} = dL_{\gamma\gamma} d\hat{\sigma}(\gamma\gamma \rightarrow X), \quad (3.8)$$

where the photon luminosity spectral function $dL_{\gamma\gamma}$ and the differential cross section $d\hat{\sigma}(\gamma\gamma \rightarrow X)$ are given from Eq. (2.12b) by

$$dL_{\gamma\gamma} = \kappa^2 L_{ee} \langle \phi_0 \phi_0 \rangle_{\tau} d\tau, \quad (3.9a)$$

$$\begin{aligned} d\hat{\sigma}(\gamma\gamma \rightarrow X) &= \frac{1}{2\hat{s}} d\Phi_X [\Sigma_{\text{unpol}} - \eta A_{\eta} \cos\phi \text{Re}(e^{-ix} \Sigma_{02}) \\ &\quad + \eta A_{\eta} \sin\phi \text{Im}(e^{-ix} \Delta_{02}) \\ &\quad + \eta^2 A_{\eta\eta} \text{Re}(e^{-2i\phi} \Sigma_{22} + e^{-2ix} \Sigma_{00})], \end{aligned} \quad (3.9b)$$

respectively. Here, κ is the e - γ conversion coefficient in the Compton backscattering and $d\Phi_X$ is the phase space factor of the final state, which is given for $X = W^+ W^-$ by

$$d\Phi_{W^+ W^-} = \frac{\hat{\beta}}{32\pi^2} d\cos\theta d\phi, \quad (3.10)$$

where $\hat{\beta} = \sqrt{1 - 4m_W^2/\hat{s}}$. The distribution (3.9b) of event rates enables us to construct two CP -odd asymmetries:

$$A_{02} = \left(\frac{2}{\pi} \right) \frac{N_{02}}{N_{\text{unpol}}}, \quad A_{00} = \frac{N_{00}}{N_{\text{unpol}}}, \quad (3.11)$$

where with $\tau_{\text{max}} = y_m^2$ and $\tau_{\text{min}} = M_X^2/s$, we have for the event distributions

$$\begin{aligned} \begin{pmatrix} N_{\text{upl}} \\ N_{02} \\ N_{00} \end{pmatrix} &= \kappa^2 L_{ee} \frac{1}{2s} \int_{\tau_{\text{min}}}^{\tau_{\text{max}}} \frac{d\tau}{\tau} \int d\Phi_X \langle \phi_0 \phi_0 \rangle_{\tau} \\ &\quad \times \begin{pmatrix} \Sigma_{\text{unpol}} \\ \eta A_{\eta} \mathcal{I}(\Sigma_{02}) \\ \eta^2 A_{\eta\eta} \mathcal{I}(\Sigma_{00}) \end{pmatrix}. \end{aligned} \quad (3.12)$$

The asymmetries depend crucially on the two-photon spectrum and the two linear polarization transfers.

We first investigate the $\sqrt{\tau}$ dependence of the two-photon spectrum and the two linear polarization transfers A_{η} and $A_{\eta\eta}$ by varying the value of the dimensionless parameter x . Three values of x are chosen; $x=0.5, 1$, and 4.83 . Two figures in Fig. 3 show clearly that the energy of two photons reaches higher ends for larger x values, but the maximum

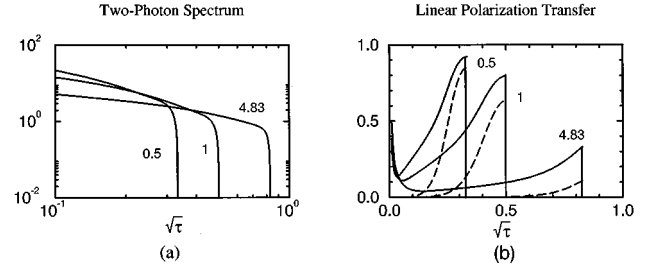


FIG. 3. (a) The $\gamma\gamma$ luminosity spectrum and (b) the two linear polarization transfers, A_{η} (solid lines) and $A_{\eta\eta}$ (dashed lines), for $x = 4E\omega_0/m_e^2 = 0.5, 1$ and 4.83 .

linear polarization transfers are larger for smaller x values. We also note that A_{η} (solid lines) is larger than $A_{\eta\eta}$ (dashed lines) in the whole range of $\sqrt{\tau}$. We should keep the parameter x as large as possible to reach higher energies. However, larger CP -odd asymmetries can be obtained for smaller x values. Therefore, there should exist a compromised value of x for the optimal observation of CP violation. The energy dependence of the subprocess cross section and that of the CP -odd asymmetries are both essential to find the optimal x value.

IV. CP -ODD WEAK-BOSON COUPLINGS

In this section we describe how CP violation from new interactions among electroweak vector bosons can be probed in a model-independent way in the W pair production in two-photon collisions. We adopt the effective Lagrangian with most general CP -odd interactions among electroweak gauge bosons. The basic assumptions are that the operators with lowest energy dimension (6) dominate the CP -odd amplitudes and that they respect the electroweak gauge invariance which is broken spontaneously by an effective $SU(2)$ -doublet scalar. The effective Lagrangian then determines the energy dependence of the scattering amplitudes at energies below the new physics scale.

A. Effective Lagrangian with CP -odd operators

The effects of new physics are parametrized by using an effective Lagrangian in a model and process independent way. As for the electroweak gauge symmetry breaking parameter, we adopt the effective $SU(2)$ -doublet scalar field Φ , which is more convenient when a physical Higgs boson appears at low energies. In addition to the Higgs doublet field Φ , the building blocks of the gauge-invariant operators are the covariant derivatives of the Higgs field, $D_{\mu}\Phi$, and the non-Abelian-field strength tensors $W_{\mu\nu}^I$ ($I=1,2,3$) and $B_{\mu\nu}$ of the $SU(2)_L$ and $U(1)_Y$ gauge fields, respectively. Considering CP -odd interactions of dimension six, we can construct six independent operators that are relevant for the process $\gamma\gamma \rightarrow W^+ W^-$:

$$\mathcal{O}_{B\tilde{B}} = g'^2 (\Phi^\dagger \Phi) B_{\mu\nu} \tilde{B}^{\mu\nu}, \quad (4.1a)$$

$$\mathcal{O}_{B\tilde{W}} = g g' (\Phi^\dagger \sigma^I \Phi) B_{\mu\nu} \tilde{W}^{I\mu\nu}, \quad (4.1b)$$

$$\mathcal{O}_{W\tilde{W}} = g^2 (\Phi^\dagger \Phi) W_{\mu\nu}^I \tilde{W}^{I\mu\nu}, \quad (4.1c)$$

$$\mathcal{O}_{\tilde{B}^-} = ig' [(D_\mu \Phi)^\dagger (D_\nu \Phi)] \tilde{B}^{\mu\nu}, \quad (4.1d)$$

$$\mathcal{O}_{\tilde{W}^-} = ig [(D_\mu \Phi)^\dagger \sigma^I (D_\nu \Phi)] \tilde{W}^{I\mu\nu}, \quad (4.1e)$$

$$\mathcal{O}_{WW\tilde{W}} = g^3 \epsilon^{IJK} \tilde{W}^{I\mu\nu} W_\nu^{J\rho} W_{\rho\mu}^K, \quad (4.1f)$$

where $\tilde{W}^{I\mu\nu} = \frac{1}{2} \epsilon^{\mu\nu\alpha\beta} W_{\alpha\beta}^I$, $\tilde{B}^{\mu\nu} = \frac{1}{2} \epsilon^{\mu\nu\alpha\beta} \tilde{B}_{\alpha\beta}$, σ^I are the Pauli matrices, and the $SU(2)_L \times U(1)_Y$ covariant derivative is given by

$$D_\mu = \partial_\mu + ig \frac{\sigma^I}{2} W_\mu^I + ig' Y B_\mu, \quad (4.2)$$

with the isospin indices I, J , and K ($= 1, 2, 3$) and the $SU(2)$ and $U(1)$ couplings, g and g' , respectively. The effective Lagrangian is written as

$$\begin{aligned} \mathcal{L} = \mathcal{L}_{\text{SM}} + \frac{1}{\Lambda^2} [& f_{B\tilde{B}} \tilde{O}_{B\tilde{B}} + f_{B\tilde{W}} \tilde{O}_{B\tilde{W}} + f_{W\tilde{W}} \tilde{O}_{W\tilde{W}} \\ & + f_{\tilde{B}} \tilde{O}_{\tilde{B}} + f_{\tilde{W}} \tilde{O}_{\tilde{W}} + f_{WW\tilde{W}} \tilde{O}_{WW\tilde{W}}], \end{aligned} \quad (4.3)$$

where the dimension-six terms \tilde{O}_i are scaled by the common dimensional parameter Λ with dimensionless coefficients f_i . The fields W^3 and B are related in terms of the Weinberg angle θ_W to the Z and photon fields, Z and A as

$$\begin{pmatrix} W^3 \\ B \end{pmatrix} = \begin{pmatrix} \cos\theta_W & \sin\theta_W \\ -\sin\theta_W & \cos\theta_W \end{pmatrix} \begin{pmatrix} Z \\ A \end{pmatrix}. \quad (4.4)$$

Incidentally, as we are interested in the photon-induced process $\gamma\gamma \rightarrow W^+W^-$, we can neglect the terms involving the Z field. Then all the terms for the process $\gamma\gamma \rightarrow W^+W^-$ can be derived by the following effective replacements

$$W_{\mu\nu}^- \rightarrow (\partial_\mu - ieA_\mu) W_\nu^- - (\partial_\nu - ieA_\nu) W_\mu^-, \quad (4.5a)$$

$$W_{\mu\nu}^+ \rightarrow (\partial_\mu + ieA_\mu) W_\nu^+ - (\partial_\nu + ieA_\nu) W_\mu^+, \quad (4.5b)$$

$$W_{\mu\nu}^3 \rightarrow \sin\theta_W F_{\mu\nu} + \frac{ie}{\sin\theta_W} (W_\mu^+ W_\nu^- - W_\nu^+ W_\mu^-), \quad (4.5c)$$

$$B_{\mu\nu} \rightarrow \cos\theta_W F_{\mu\nu}, \quad (4.5d)$$

where $F_{\mu\nu} = \partial_\mu A_\nu - \partial_\nu A_\mu$. We take the unitary gauge, where the scalar doublet Φ with hypercharge $Y = \frac{1}{2}$ takes the form

$$\Phi = \frac{1}{\sqrt{2}} (v + H) \begin{bmatrix} 0 \\ 1 \end{bmatrix}. \quad (4.6)$$

H denotes the Higgs boson in the SM. It is now straightforward to obtain the new CP -odd vertices among terms of the component fields, W^\pm , A , and H in the unitary gauge.

B. CP -odd vertices

In this section we give the Feynman rules for the γWW , $\gamma\gamma H$, HWW , and $\gamma\gamma WW$ vertices, relevant for the $\gamma\gamma \rightarrow W^+W^-$ reaction. Table II shows which vertices exist already in the SM at tree level and which new vertices appear from the new dimension-six CP -odd operators. Firstly, the three operators, $\mathcal{O}_{B\tilde{B}}$, $\mathcal{O}_{B\tilde{W}}$, and $\mathcal{O}_{W\tilde{W}}$ contribute to the

TABLE II. Vertices relevant for the process $\gamma\gamma \rightarrow W^+W^-$ in the SM with dimension-six CP -odd terms.

Vertex	γWW	$\gamma\gamma WW$	HWW	$\gamma\gamma H$
SM	○	○	○	×
$\mathcal{O}_{B\tilde{B}}$	×	×	×	○
$\mathcal{O}_{B\tilde{W}}$	○	×	×	○
$\mathcal{O}_{W\tilde{W}}$	×	×	○	○
$\mathcal{O}_{\tilde{B}}$	○	×	×	×
$\mathcal{O}_{\tilde{W}}$	○	×	○	×
$\mathcal{O}_{WW\tilde{W}}$	○	○	×	×

$\gamma\gamma H$ vertex. Secondly, we find that the operator $\mathcal{O}_{WW\tilde{W}}$ gives a new CP -odd γWW vertex and a new CP -odd $\gamma\gamma WW$ vertex, which are related by $U(1)$ electromagnetic gauge invariance. In addition, the three operators, $\mathcal{O}_{B\tilde{W}}$, $\mathcal{O}_{\tilde{W}}$, and $\mathcal{O}_{\tilde{B}}$ contribute to the γWW vertex as well. Thirdly, we find that $\mathcal{O}_{W\tilde{W}}$ and $\mathcal{O}_{\tilde{W}}$ contribute to the HWW vertex.

For convenience, we define four new dimensionless form factors, Y_i ($i = 1$ to 4), which are related with the coefficients, f_i 's ($i = B\tilde{B}, B\tilde{W}, W\tilde{W}, \tilde{B}, \tilde{W}, WW\tilde{W}$) as

$$\begin{aligned} Y_1 &= \left(\frac{m_W}{\Lambda}\right)^2 \left[f_{B\tilde{W}} + \frac{1}{4} f_{\tilde{B}} + f_{\tilde{W}} \right], & Y_2 &= \left(\frac{m_W}{\Lambda}\right)^2 \frac{g^2}{4} f_{WW\tilde{W}}, \\ Y_3 &= \left(\frac{m_W}{\Lambda}\right)^2 \left[f_{W\tilde{W}} + \frac{1}{4} f_{\tilde{W}} \right], \\ Y_4 &= \left(\frac{m_W}{\Lambda}\right)^2 [f_{B\tilde{B}} - f_{B\tilde{W}} - f_{W\tilde{W}}]. \end{aligned} \quad (4.7)$$

If all the coefficients, f_i , are of the similar size, then Y_2 would be about ten times smaller than the other form factors in size because of the factor $g^2/4 \sim 0.1$. We denote the Feynman rule of a vertex V in the form; $ie\Gamma_V$. It is then straightforward to derive the explicit form of two simple $\gamma\gamma H$ and HWW vertices:

$$\Gamma_{\gamma\gamma H}^{\mu\nu}(k_1, k_2) = \frac{8Y_4}{m_W} \sin\theta_W \epsilon^{\mu\nu\rho\sigma} k_{1\rho} k_{2\sigma}, \quad (4.8)$$

$$\Gamma_{HWW}^{\alpha\beta}(q_1, q_2) = \frac{m_W}{\sin\theta_W} g^{\alpha\beta} + \frac{8Y_3}{m_W \sin\theta_W} \epsilon^{\alpha\beta\rho\sigma} q_{1\rho} q_{2\sigma}, \quad (4.9)$$

where $k_1(\mu)$ and $k_2(\nu)$ are four-momenta (Lorentz indices) of two incoming photons and $q_1(\alpha)$ and $q_2(\beta)$ are four-momenta (Lorentz indices) for the outgoing W^+ and W^- , respectively. In the SM the $\gamma\gamma H$ vertex appears in the one-loop level, we do not study its consequences in this paper. The triple γWW vertex is

$$\begin{aligned} \Gamma_{\gamma WW}^{\mu\alpha\beta}(k, q_1, q_2) &= (q_1 - q_2)^\mu g^{\alpha\beta} - (q_1 + k)^\beta g^{\mu\alpha} + (k + q_2)^\alpha g^{\mu\beta} \\ &\quad - 4Y_1 \epsilon^{\mu\alpha\beta\rho} k_\rho + 12 \frac{Y_2}{m_W^2} [2(q_1 \cdot q_2) \epsilon^{\mu\alpha\beta\rho} \\ &\quad - q_2^\alpha \epsilon^{\mu\beta\rho\sigma} (q_1 - q_2)_\sigma - q_1^\beta \epsilon^{\mu\alpha\rho\sigma} (q_1 - q_2)_\sigma] k_\rho, \end{aligned} \quad (4.10)$$

where $k = q_1 + q_2$, and the quartic $\gamma\gamma WW$ vertex is

$$\begin{aligned} \Gamma_{\gamma\gamma WW}^{\mu\nu\alpha\beta}(k_1, k_2, q_1, q_2) = & -2g^{\mu\nu}g^{\alpha\beta} + g^{\mu\alpha}g^{\nu\beta} + g^{\mu\beta}g^{\nu\alpha} + 8\frac{Y_2}{m_W^2} [2g^{\alpha\beta}\epsilon^{\mu\nu\rho\sigma}k_{1\rho}k_{2\sigma} + 2g^{\mu\nu}\epsilon^{\alpha\beta\rho\sigma}q_{1\rho}q_{2\sigma} - g^{\mu\alpha}\epsilon^{\nu\beta\rho\sigma}q_{2\rho}k_{2\sigma} \\ & - g^{\mu\beta}\epsilon^{\nu\alpha\rho\sigma}q_{1\rho}k_{2\sigma} - g^{\nu\alpha}\epsilon^{\mu\beta\rho\sigma}q_{2\rho}k_{1\sigma} - g^{\nu\beta}\epsilon^{\mu\alpha\rho\sigma}q_{1\rho}k_{1\sigma} + (k_1 - k_2)(q_1 - q_2)\epsilon^{\mu\nu\alpha\beta} + k_2^\mu\epsilon^{\nu\alpha\beta\rho}(q_1 \\ & - q_2)_\rho + k_1^\nu\epsilon^{\mu\alpha\beta\rho}(q_1 - q_2)_\rho + q_2^\alpha\epsilon^{\mu\nu\beta\rho}(k_1 - k_2)_\rho + q_1^\beta\epsilon^{\mu\nu\alpha\rho}(k_1 - k_2)_\rho + (q_1 - q_2)^\mu\epsilon^{\nu\alpha\beta\rho}(k_1 + k_2)_\rho \\ & + (q_1 - q_2)^\nu\epsilon^{\mu\alpha\beta\rho}(k_1 + k_2)_\rho + (k_1 - k_2)^\alpha\epsilon^{\mu\nu\beta\rho}(q_1 + q_2)_\rho + (k_1 - k_2)^\beta\epsilon^{\mu\nu\alpha\rho}(q_1 + q_2)_\rho]. \end{aligned} \quad (4.11)$$

V. HELICITY AMPLITUDES FOR $\gamma\gamma \rightarrow W^+ W^-$

In this section we present the complete calculation of polarization amplitudes for the process

$$\gamma(k_1, \lambda_1) + \gamma(k_2, \lambda_2) \rightarrow W^+(q_1, \lambda_3) + W^-(q_2, \lambda_4), \quad (5.1)$$

with the effective Lagrangian (4.3) in Sec. IV. The four-momentum and the helicity of each particle are shown in the parentheses. The helicities of the W are given in the $\gamma\gamma$ c.m. frame. Helicity amplitudes contain full information of the process. The relative phases of the amplitudes are essential because the interference of different photon and W helicity states gives a nontrivial azimuthal-angle dependence.

By taking the two photon momenta along the z axis and by taking the W^+ momentum in the x - z plane (see Fig. 1), the four-momenta are parametrized as

$$\begin{aligned} k_1^\mu &= \frac{\sqrt{\hat{s}}}{2}(1, 0, 0, 1), & k_2^\mu &= \frac{\sqrt{\hat{s}}}{2}(1, 0, 0, -1), \\ q_1^\mu &= \frac{\sqrt{\hat{s}}}{2}(1, \hat{\beta}\sin\theta, 0, \hat{\beta}\cos\theta), \\ q_2^\mu &= \frac{\sqrt{\hat{s}}}{2}(1, -\hat{\beta}\sin\theta, 0, -\hat{\beta}\cos\theta). \end{aligned} \quad (5.2)$$

The incoming photon polarization vectors are

$$\epsilon_1^\mu(\pm) = \mp \frac{1}{\sqrt{2}}(0, 1, \pm i, 0), \quad \epsilon_2^\mu(\pm) = \mp \frac{1}{\sqrt{2}}(0, 1, \mp i, 0), \quad (5.3)$$

and the transverse (helicity- ± 1) and longitudinal (helicity-0) polarization vectors of the W^\pm bosons are

$$\begin{aligned} \epsilon_3^{*\mu}(\pm) &= \mp \frac{1}{\sqrt{2}}(0, \cos\theta, \mp i, -\sin\theta), \\ \epsilon_4^{*\mu}(\pm) &= \mp \frac{1}{\sqrt{2}}(0, -\cos\theta, \mp i, \sin\theta), \\ \epsilon_3^{*\mu}(0) &= \frac{\sqrt{\hat{s}}}{2m_W}(\hat{\beta}, \sin\theta, 0, \cos\theta), \end{aligned}$$

$$\epsilon_4^{*\mu}(0) = \frac{\sqrt{\hat{s}}}{2m_W}(\hat{\beta}, -\sin\theta, 0, -\cos\theta), \quad (5.4)$$

respectively.

The helicity amplitudes then can be parametrized as

$$\tilde{\mathcal{M}}_{\lambda_1\lambda_2;\lambda_3\lambda_4}(\theta) = e^2 \tilde{\mathcal{M}}_{\lambda_1\lambda_2;\lambda_3\lambda_4}(\theta) d_{\Delta\lambda_{12}, \Delta\lambda_{34}}^{J_0}, \quad (5.5)$$

where $\Delta\lambda_{12} = \lambda_1 - \lambda_2$, $\Delta\lambda_{34} = \lambda_3 - \lambda_4$, $J_0 = \max(|\Delta\lambda_{12}|, |\Delta\lambda_{34}|)$, and $d_{\Delta\lambda_{12}, \Delta\lambda_{34}}^{J_0}$ is the d function. The explicit form of the d functions needed here is listed in Table III.

We separate the amplitude into the SM contribution and the new CP -odd contributions with the factor i extracted

$$\tilde{\mathcal{M}} = \tilde{\mathcal{M}}_{\text{SM}} + i\tilde{\mathcal{M}}_N, \quad (5.6)$$

where the new contribution can be decomposed in the form

$$\tilde{\mathcal{M}}_N = Y_1 \tilde{\mathcal{M}}^{Y_1} + Y_2 \tilde{\mathcal{M}}^{Y_2} + Y_3 \tilde{\mathcal{M}}^{Y_3} + Y_4 \tilde{\mathcal{M}}^{Y_4}. \quad (5.7)$$

Here we retain only those terms with one insertion of CP -odd operators.

A. The standard model amplitudes

The process $\gamma\gamma \rightarrow W^+ W^-$ is P - and CP -preserving in the SM at the tree level. This leads to the following relations

$$\begin{aligned} P: \quad \tilde{\mathcal{M}}_{\lambda_1\lambda_2;\lambda_3\lambda_4} &= \tilde{\mathcal{M}}_{-\lambda_1, -\lambda_2; -\lambda_3, -\lambda_4}, \\ CP: \quad \tilde{\mathcal{M}}_{\lambda_1\lambda_2;\lambda_3\lambda_4} &= \tilde{\mathcal{M}}_{-\lambda_2, -\lambda_1; -\lambda_4, -\lambda_3}. \end{aligned} \quad (5.8)$$

The Bose symmetry leads to the relation

$$\tilde{\mathcal{M}}_{\lambda_1\lambda_2;\lambda_3\lambda_4} = \tilde{\mathcal{M}}_{\lambda_2\lambda_1;\lambda_3\lambda_4}(\cos\theta \rightarrow -\cos\theta). \quad (5.9)$$

TABLE III. Explicit form of the d functions needed.

$$\begin{aligned} d_{2,2}^2(\theta) &= d_{-2,-2}^2(\theta) = \frac{1}{4}(1 + \cos\theta)^2 \\ d_{2,-2}^2(\theta) &= d_{-2,2}^2(\theta) = \frac{1}{4}(1 - \cos\theta)^2 \\ d_{2,1}^2(\theta) &= -d_{-2,-1}^2(\theta) = -\frac{1}{2}(1 + \cos\theta)\sin\theta \\ d_{2,-1}^2(\theta) &= -d_{-2,1}^2(\theta) = \frac{1}{2}(1 - \cos\theta)\sin\theta \\ d_{2,0}^2(\theta) &= d_{-2,0}^2(\theta) = d_{0,2}^2(\theta) = d_{0,-2}^2(\theta) = \sqrt{\frac{3}{8}}\sin^2\theta \\ d_{0,1}^1(\theta) &= d_{0,-1}^1(\theta) = \sqrt{\frac{1}{2}}\sin\theta \\ d_{0,0}^0(\theta) &= 1 \end{aligned}$$

Let us rewrite the amplitude in the form

$$\tilde{\mathcal{M}}_{\text{SM}} = \frac{\tilde{\mathcal{N}}^{\text{SM}}}{1 - \hat{\beta}^2 \cos^2 \theta}, \quad (5.10)$$

by extracting the t - and u -channel W boson propagator factor. It is clear that the coefficients $\tilde{\mathcal{N}}^{\text{SM}}$ s satisfy the same P , CP -, and Bose-symmetry relations as $\tilde{\mathcal{M}}_{\text{SM}}$. We find for the positive photon helicity ($\lambda_1 = +$),

$$\begin{aligned} \tilde{\mathcal{N}}_{+++; ++}^{\text{SM}} &= 2(1 + \hat{\beta})^2, & \tilde{\mathcal{N}}_{+++; +0}^{\text{SM}} &= \tilde{\mathcal{N}}_{+++; +-}^{\text{SM}} = \tilde{\mathcal{N}}_{+++; 0+}^{\text{SM}} = 0, \\ \tilde{\mathcal{N}}_{+++; 00}^{\text{SM}} &= -\frac{8}{\hat{r}}, & \tilde{\mathcal{N}}_{+++; 0-}^{\text{SM}} &= \tilde{\mathcal{N}}_{+++; -+}^{\text{SM}} = \tilde{\mathcal{N}}_{+++; -0}^{\text{SM}} = 0, \\ \tilde{\mathcal{N}}_{++--; --}^{\text{SM}} &= 2(1 - \hat{\beta})^2, & \tilde{\mathcal{N}}_{+-; ++}^{\text{SM}} &= \frac{32}{\sqrt{6}\hat{r}}, & \tilde{\mathcal{N}}_{+-; +-}^{\text{SM}} &= 8, \\ \tilde{\mathcal{N}}_{+-; +0}^{\text{SM}} &= \tilde{\mathcal{N}}_{+-; 0+}^{\text{SM}} = \frac{8}{\sqrt{2}\hat{r}}, & \tilde{\mathcal{N}}_{+-; 00}^{\text{SM}} &= 4\sqrt{\frac{2}{3}}(2 - \hat{\beta}^2), \end{aligned} \quad (5.11)$$

where $\hat{r} = \hat{s}/m_W^2$. The other remaining coefficients can be obtained by using the P and CP relations (5.8) and the Bose symmetry. We note the following three features of the SM amplitudes.

The amplitudes for producing two W 's with the nonvanishing total spin component along the W boson momentum direction ($\Delta\lambda_{34}$) vanish when the initial state has $J_z = \Delta\lambda_{12} = 0$.

The amplitude for producing two longitudinal W 's from a $J_z = 0$ initial state is suppressed by a factor of $1/\hat{r}$ in the SM. The same behavior should appear in the production of two charged scalars such as $\gamma\gamma \rightarrow \pi^+ \pi^-$.

The amplitudes for producing two right-(left-)handed W 's from two left-(right-)handed photons is suppressed by a factor of $1/\hat{r}^2$. The results are consistent with those by Yehudai [4] and by Bélanger *et al.* [9].

B. CP -odd amplitudes

Every CP -odd amplitude and its CP -conjugate amplitude satisfy the following relation

$$\tilde{\mathcal{M}}_{\lambda_1 \lambda_2; \lambda_3 \lambda_4}^{Y_i} = -\tilde{\mathcal{M}}_{-\lambda_2, -\lambda_1; -\lambda_4, -\lambda_3}^{Y_i} \quad (i=1,2,3,4), \quad (5.12)$$

since the factor of i is extracted in the full helicity amplitude (5.6). It then follows that any CP self-conjugate amplitude has a vanishing contribution from the CP -odd terms:

$$\begin{aligned} \tilde{\mathcal{M}}^{Y_i}(\pm\mp; \pm\mp) &= \tilde{\mathcal{M}}^{Y_i}(\pm\mp; \mp\pm) = \tilde{\mathcal{M}}^{Y_i}(\pm\mp; 00) = 0 \\ & \quad (i=1,2,3,4). \end{aligned} \quad (5.13)$$

The Y_1 and Y_2 terms contribute to the t and u channels and Y_2 contributes to the contact $\gamma\gamma WW$ diagram as well. By using the notation

$$\tilde{\mathcal{M}}^{Y_i} = \frac{\tilde{\mathcal{N}}^{Y_i}}{1 - \hat{\beta}^2 \cos^2 \theta} \quad (i=1,2), \quad (5.14)$$

we find that the nonvanishing Y_1 contributions are

$$\begin{aligned} \tilde{\mathcal{N}}_{+++; ++}^{Y_1} &= -\tilde{\mathcal{N}}_{---; --}^{Y_1} = 8[2 + \hat{\beta}(1 + \cos^2 \theta)], \\ \tilde{\mathcal{N}}_{+++; +0}^{Y_1} &= -\tilde{\mathcal{N}}_{---; 0-}^{Y_1} = \tilde{\mathcal{N}}_{+++; 0+}^{Y_1} = -\tilde{\mathcal{N}}_{---; -0}^{Y_1} \\ &= 4\sqrt{\hat{r}}\hat{\beta}(1 + \hat{\beta}), \\ \tilde{\mathcal{N}}_{+++; 00}^{Y_1} &= -\tilde{\mathcal{N}}_{---; 00}^{Y_1} = -4\hat{r}(1 - \hat{\beta}^2 \cos^2 \theta), \\ \tilde{\mathcal{N}}_{+++; 0-}^{Y_1} &= -\tilde{\mathcal{N}}_{---; +0}^{Y_1} = \tilde{\mathcal{N}}_{+++; -0}^{Y_1} = -\tilde{\mathcal{N}}_{---; 0+}^{Y_1} \\ &= -4\sqrt{\hat{r}}\hat{\beta}(1 - \hat{\beta}), \\ \tilde{\mathcal{N}}_{+++; -+}^{Y_1} &= -\tilde{\mathcal{N}}_{---; ++}^{Y_1} = 8[2 - \hat{\beta}(1 + \cos^2 \theta)], \\ \tilde{\mathcal{N}}_{+-; ++}^{Y_1} &= -\tilde{\mathcal{N}}_{+-; --}^{Y_1} = \tilde{\mathcal{N}}_{-+; ++}^{Y_1} = -\tilde{\mathcal{N}}_{-+; --}^{Y_1} = -\frac{32}{\sqrt{6}}\hat{\beta}, \\ \tilde{\mathcal{N}}_{+-; +0}^{Y_1} &= -\tilde{\mathcal{N}}_{+-; 0-}^{Y_1} = \tilde{\mathcal{N}}_{+-; 0+}^{Y_1} = -\tilde{\mathcal{N}}_{+-; -0}^{Y_1} = \tilde{\mathcal{N}}_{-+; +0}^{Y_1} \\ &= -\tilde{\mathcal{N}}_{-+; 0-}^{Y_1} = \tilde{\mathcal{N}}_{-+; 0+}^{Y_1} = -\tilde{\mathcal{N}}_{-+; -0}^{Y_1} = -4\sqrt{2}\hat{r}\hat{\beta}, \end{aligned} \quad (5.15)$$

and the nonvanishing Y_2 contributions are

$$\begin{aligned} \tilde{\mathcal{N}}_{+++; ++}^{Y_2} &= -\tilde{\mathcal{N}}_{---; --}^{Y_2} = -12\hat{r}[1 - 3\hat{\beta} + \hat{\beta}^2 + \hat{\beta}^3 \\ & \quad + (1 + \hat{\beta} - 3\hat{\beta}^2 + \hat{\beta}^3)\cos^2 \theta], \\ \tilde{\mathcal{N}}_{+++; +0}^{Y_2} &= -\tilde{\mathcal{N}}_{---; 0-}^{Y_2} = \tilde{\mathcal{N}}_{+++; 0+}^{Y_2} = -\tilde{\mathcal{N}}_{---; -0}^{Y_2} \\ &= -24\sqrt{\hat{r}}(\hat{\beta} + 1)(\hat{\beta} - 2)\cos \theta, \\ \tilde{\mathcal{N}}_{+++; +-}^{Y_2} &= -\tilde{\mathcal{N}}_{---; +-}^{Y_2} = \tilde{\mathcal{N}}_{+++; -+}^{Y_2} = -\tilde{\mathcal{N}}_{---; -+}^{Y_2} \\ &= -\frac{48}{\sqrt{6}}\hat{r}(1 + \hat{\beta}^2), \\ \tilde{\mathcal{N}}_{+++; 00}^{Y_2} &= -\tilde{\mathcal{N}}_{---; 00}^{Y_2} = 96\sin^2 \theta, \\ \tilde{\mathcal{N}}_{+++; 0-}^{Y_2} &= -\tilde{\mathcal{N}}_{---; +0}^{Y_2} = \tilde{\mathcal{N}}_{+++; -0}^{Y_2} = -\tilde{\mathcal{N}}_{---; 0+}^{Y_2} \\ &= 24\sqrt{\hat{r}}(\hat{\beta} - 1)(\hat{\beta} + 2)\cos \theta, \\ \tilde{\mathcal{N}}_{+++; -+}^{Y_2} &= -\tilde{\mathcal{N}}_{---; ++}^{Y_2} = -12\hat{r}[1 + 3\hat{\beta} + \hat{\beta}^2 - \hat{\beta}^3 \\ & \quad + (1 - \hat{\beta} - 3\hat{\beta}^2 - \hat{\beta}^3)\cos^2 \theta], \\ \tilde{\mathcal{N}}_{+-; ++}^{Y_2} &= -\tilde{\mathcal{N}}_{+-; --}^{Y_2} = \tilde{\mathcal{N}}_{-+; ++}^{Y_2} = -\tilde{\mathcal{N}}_{-+; --}^{Y_2} \\ &= \frac{48}{\sqrt{6}}\hat{r}(1 + \hat{\beta}^2), \end{aligned}$$

$$\begin{aligned}
\tilde{\mathcal{N}}_{+-;+0}^{Y_2} &= -\tilde{\mathcal{N}}_{+-;0-}^{Y_2} = \tilde{\mathcal{N}}_{+-;0+}^{Y_2} = -\tilde{\mathcal{N}}_{+-;-0}^{Y_2} \\
&= \tilde{\mathcal{N}}_{-+;+0}^{Y_2} = -\tilde{\mathcal{N}}_{-+;0-}^{Y_2} = \tilde{\mathcal{N}}_{-+;0+}^{Y_2} = -\tilde{\mathcal{N}}_{-+;-0}^{Y_2} \\
&= 24\sqrt{2}\hat{r}\hat{\beta}. \tag{5.16}
\end{aligned}$$

The two contributions behave differently at high energies. The Y_1 contributions are dominant in the amplitudes for producing two longitudinal W 's from the $J_Z=0$ initial photon state

$$\tilde{\mathcal{N}}_{\pm\pm;00}^{Y_1} \rightarrow \mp 4\hat{r}\sin^2\theta, \tag{5.17}$$

while the Y_2 contributions are dominant in the amplitudes for producing two transverse W 's except for the $(\pm\pm;\pm\pm)$ modes

$$\begin{aligned}
\tilde{\mathcal{N}}_{\pm\pm;\mp\mp}^{Y_2} &\rightarrow \mp 48\hat{r}\sin^2\theta, \\
\tilde{\mathcal{N}}_{\pm\pm;+-}^{Y_2} = \tilde{\mathcal{N}}_{\pm\pm;-+}^{Y_2} &\rightarrow \mp 16\sqrt{6}\hat{r}, \\
\tilde{\mathcal{N}}_{+-;\pm\pm}^{Y_2} = \tilde{\mathcal{N}}_{-+;\pm\pm}^{Y_2} &\rightarrow \pm 16\sqrt{6}\hat{r}. \tag{5.18}
\end{aligned}$$

The high-energy behavior of two sets of amplitudes (5.15) and (5.16) are in sharp contrast to that of the SM amplitudes whose dominant contributions are in the $(\pm\pm;\pm\pm)$, $(\pm\mp;\pm\mp)$, and $(\pm\mp;00)$ modes. Because of this, interference between different helicity amplitudes are essential for observing significant CP -violation effects. Use of the linearly polarized photon beams allow us to study interference between the leading CP -even (SM) amplitudes and the leading CP -odd amplitudes. In our approximation of neglecting the one-loop $\gamma\gamma H$ vertex of the SM, there is no contribution from the Y_3 term;

$$\tilde{\mathcal{M}}^{Y_3} = 0. \tag{5.19}$$

On the other hand, Y_4 contributes to the s -channel scalar exchange diagram in the helicity amplitudes with $\Delta\lambda_{12}=\Delta\lambda_{34}=0$. An explicit calculation shows that the non-vanishing amplitudes, $\tilde{\mathcal{M}}_{Y_4}$, are as follows:

$$\begin{aligned}
\tilde{\mathcal{M}}_{++++}^{Y_4} &= -\tilde{\mathcal{M}}_{----}^{Y_4} = 4\chi_H(\hat{s}), \\
\tilde{\mathcal{M}}_{++;00}^{Y_4} &= -\tilde{\mathcal{M}}_{--;00}^{Y_4} = -\hat{r}(1+\hat{\beta}^2)\chi_H(\hat{s}), \\
\tilde{\mathcal{M}}_{+-;--}^{Y_4} &= -\tilde{\mathcal{M}}_{-+;+-}^{Y_4} = 4\chi_H(\hat{s}), \tag{5.20}
\end{aligned}$$

where χ_H is the Higgs propagator factor

$$\chi_H(\hat{s}) = \frac{\hat{s}}{\hat{s} - m_H^2 + im_H\Gamma_H}. \tag{5.21}$$

In the subsequent numerical studies, we examine the case with $m_H=100$ GeV, where the width Γ_H is safely neglected. We will study the $m_H \geq 2m_W$ case elsewhere, since there both the tree- and one-loop SM amplitudes are relevant.

VI. DIFFERENTIAL CROSS SECTION

In counting experiments where the final W polarizations are not analyzed, we measure only the following combinations:

$$\sum_X M_{\lambda_1\lambda_2} M_{\lambda'_1\lambda'_2}^* = e^4 \sum_{\lambda_3} \sum_{\lambda_4} \tilde{\mathcal{M}}_{\lambda_1\lambda_2;\lambda_3\lambda_4} \tilde{\mathcal{M}}_{\lambda'_1\lambda'_2;\lambda_3\lambda_4}^*. \tag{6.1}$$

We then find Σ_{unpol} , Σ_{02} , Δ_{02} , Σ_{22} , and Σ_{00} from Eqs. (2.13). The differential cross section for a fixed angle χ is

$$\begin{aligned}
\frac{d^2\sigma}{d\cos\theta d\phi}(\chi) &= \frac{\alpha^2}{8\hat{s}(1-\hat{\beta}^2\cos^2\theta)^2} \left\{ \hat{\Sigma}_{\text{unpol}} - \frac{1}{2}\text{Re}[(\eta e^{-i(\chi+\phi)} \right. \\
&\quad \left. + \bar{\eta} e^{-i(\chi-\phi)})\hat{\Sigma}_{02}] + \frac{1}{2}\text{Re}[(\eta e^{-i(\chi+\phi)} \right. \\
&\quad \left. - \bar{\eta} e^{-i(\chi-\phi)})\hat{\Delta}_{02}] + \eta\bar{\eta}\text{Re}(e^{-2i\phi}\hat{\Sigma}_{22}) \right. \\
&\quad \left. + e^{-2i\chi}\hat{\Sigma}_{00} \right\}, \tag{6.2}
\end{aligned}$$

$$\Sigma_i = \frac{e^2\hat{\Sigma}_i}{(1-\hat{\beta}^2\cos^2\theta)^2}, \quad \Delta_{02} = \frac{e^2\hat{\Delta}_{02}}{(1-\hat{\beta}^2\cos^2\theta)^2}, \tag{6.3}$$

for $i=\text{unpol}, 02, 22$, and 00 .

We first note that all the real parts of the distributions (6.1) are independent of the anomalous CP -odd form factors Y_i up to linear order

$$\hat{\Sigma}_{\text{unpol}} = 38 - 4\hat{\beta}^2(3 - 8\cos^2\theta) + 6\hat{\beta}^4(1 + \sin^4\theta),$$

$$\mathcal{R}(\hat{\Sigma}_{02}) = \frac{96}{\hat{r}}\hat{\beta}^2\sin^2\theta, \quad \mathcal{R}(\hat{\Delta}_{00}) = 0,$$

$$\mathcal{R}(\hat{\Sigma}_{22}) = 6\hat{\beta}^4\sin^4\theta, \quad \mathcal{R}(\hat{\Sigma}_{00}) = \frac{96}{\hat{r}^2}. \tag{6.4}$$

On the other hand, two CP -odd distributions, $\mathcal{I}(\hat{\Sigma}_{02})$ and $\mathcal{I}(\hat{\Sigma}_{00})$, have contributions from the Y_1 , Y_2 , and Y_4 terms

$$\begin{aligned}
\mathcal{I}(\hat{\Sigma}_{02}) &= -4\hat{r}\hat{\beta}^2[4(1-\hat{\beta}^2\cos^2\theta)R(Y_1) \\
&\quad + 48(3+\hat{\beta}^2\cos^2\theta)R(Y_2) + (5-3\hat{\beta}^2) \\
&\quad \times (1-\hat{\beta}^2\cos^2\theta)R(Y_4\chi_H)]\sin^2\theta, \tag{6.5}
\end{aligned}$$

$$\begin{aligned}
\mathcal{I}(\hat{\Sigma}_{00}) &= 24[4R(Y_1) - 4\hat{r}(1+3\hat{\beta}^2)R(Y_2) \\
&\quad + (1+\hat{\beta}^2)R(Y_4\chi_H)](1-\hat{\beta}^2\cos^2\theta). \tag{6.6}
\end{aligned}$$

A few comments on the CP -odd distributions are in order.

(i) $\mathcal{I}(\hat{\Sigma}_{02})$ has $\hat{\beta}^2$ as an overall factor such that the contribution vanishes at the threshold, whereas $\mathcal{I}(\hat{\Sigma}_{00})$ does not.

(ii) Both CP -odd distributions have the angular terms ($\sin^2\theta$ and $1-\hat{\beta}^2\cos^2\theta$) which become largest at the scatter-

ing angle $\theta=\pi/2$, where the SM contributions are generally small. We, therefore, expect large CP -odd asymmetries at $\theta\approx\pi/2$.

(iii) Each term in $\mathcal{I}(\Sigma_{02})$ has a different angular dependence which allows us to disentangle them. On the other hand, we note that all the terms in the $\mathcal{I}(\Sigma_{00})$ mode have the same angular dependence. The only way to distinguish them is to study its energy dependence. We show that this can be done efficiently by adjusting the laser beam frequency in the Compton backscattering mode.

(iv) At high energies ($\hat{s}\gg 1$), $R(Y_1)$, and $R(Y_4)$ are measured from $\mathcal{I}(\Sigma_{02})$, whereas $R(Y_2)$ affects both $\mathcal{I}(\Sigma_{00})$ and $\mathcal{I}(\Sigma_{02})$.

VII. OBSERVABLE CONSEQUENCES OF CP -ODD COUPLINGS

Let us estimate the various experimental branching fractions of W decays. Consider the decay of each W into a fermion-antifermion pair (quark-antiquark $q_1\bar{q}_2$ or charged lepton-neutrino $l\nu_l$) at the tree level. The branching ratio for $W^-\rightarrow l\bar{\nu}_l$ ($l=e,\mu,$ or τ) is about 10% each [20]. We thus expect the following final state combinations:

$$\begin{aligned} (q\bar{q})(q\bar{q}) &\Rightarrow 4\text{jets} \quad 49\%, \\ (q\bar{q})(l\nu) &\Rightarrow \text{dijet}+l^\pm+\not{p} \quad 42\%, \\ (l\bar{\nu})(\bar{l}\nu) &\Rightarrow l^+l^-+\not{p} \quad 9\%, \end{aligned} \quad (7.1)$$

where \not{p} stands for the momentum of the escaping neutrino(s). The dijet+ l^\pm mode is most amenable for W -spin analysis. In our analysis, no spin analysis for the decaying W 's is required. In case of $\mathcal{I}(\Sigma_{00})$, not even the scattering plane needs to be identified. Even if one excludes the $\tau^+\tau^-+\not{p}$ modes of 1%, the remaining 99% of the events can be used to measure $\mathcal{I}(\Sigma_{00})$. On the other hand, the scattering plane should be identified to measure $\mathcal{I}(\Sigma_{02})$. It is worth noting that the charge of the decaying W is not needed to extract $\mathcal{I}(\Sigma_{02})$. Therefore, all the modes except for the $l^+l^-+\not{p}$ modes (9%) can be used for $\mathcal{I}(\Sigma_{02})$.

Certainly, a realistic experimental analysis should include all the possible background processes and consider all the available experimental cuts in order to reduce those backgrounds. The heavy fermion-pair production processes such as $\gamma\gamma\rightarrow t\bar{t}$, $\gamma\gamma\rightarrow b\bar{b}$, and $\gamma\gamma\rightarrow\tau\bar{\tau}$ can spoil the $\gamma\gamma\rightarrow W^+W^-$ process. However, we note that the $\gamma\gamma\rightarrow W^+W^-$ reaction has a much larger cross section than those heavy fermion-pair production processes. Furthermore, the total cross section increases to a constant value at high c.m. energies. At $\sqrt{s}=500$ GeV the total cross section is about 80 pb, while the heavy fermion-pair production cross section is of the order of 1 pb. So we expect that there do not exist very serious background problems. In the present work we simply use all the W pair events. It would be rather straightforward to include the effects from any experimental cuts and efficiencies in addition to the branching factors discussed above.

We present our numerical analysis at the following set of collider parameters:

$$\sqrt{s}=0.5 \text{ and } 1.0 \text{ TeV}, \quad \kappa^2 L_{ee}=20 \text{ fb}^{-1}. \quad (7.2)$$

The dimensionless parameter x , which is dependent on the laser frequency ω_0 , is treated as an adjustable parameter. We note that $\kappa=1$ is the maximally allowed value for the e - γ conversion coefficient κ and it may be as small as $\kappa=0.1$ if the collider is optimized for the e^+e^- mode [15]. All one should note is that the significance of the signal scales as $(\epsilon\kappa^2 L_{ee})$, where ϵ denotes the overall detection efficiency that is different for A_{00} and A_{02} .

A. Statistical significance of possible signals

The two CP -odd integrated asymmetries, A_{00} and A_{02} , depend linearly on the form factors, $R(Y_1)$, $R(Y_2)$, and $R(Y_4)$ in the approximation that only the terms linear in the form factors are retained. We present the sensitivities to each form factor, assuming that the other form factors are zero. The analyses are cataloged into two parts: the $\gamma(\gamma)WW$ part and the $\gamma\gamma H$ part.

Folding the photon luminosity spectrum and integrating the distributions over the polar angle θ , we obtain the x dependence of available event rates:

$$\begin{aligned} \begin{pmatrix} N_{\text{unpol}} \\ N_{02} \\ N_{00} \end{pmatrix} &= \kappa^2 L_{ee} \frac{\pi\alpha^2}{2s} \int_{\tau_{\min}}^{\tau_{\max}} \frac{d\tau}{\tau} \int_{-1}^1 d\cos\theta \\ &\times \frac{\hat{\beta}\langle\phi_0\phi_0\rangle_\tau}{(1-\hat{\beta}^2\cos^2\theta)^2} \begin{pmatrix} \hat{\Sigma}_{\text{unpol}} \\ A_\eta\mathcal{I}(\hat{\Sigma}_{02}) \\ A_\eta\mathcal{I}(\hat{\Sigma}_{00}) \end{pmatrix}, \end{aligned} \quad (7.3)$$

where $\tau_{\max}=[x/(1+x)]^2$ and $\tau_{\min}=4m_W^2/s$. One measure of the significance of a CP -odd asymmetry is the standard deviation $\tilde{\mathcal{N}}_{SD}^a$ by which the asymmetry exceeds the expected statistical fluctuation of the background distribution; for $a=02$ and 00

$$\tilde{\mathcal{N}}_{SD}^a = \frac{|A_a|}{\sqrt{2/\epsilon N_{\text{unpol}}}}. \quad (7.4)$$

Here ϵ is for the sum of W branching fractions available, which is taken to be

$$\epsilon = \begin{cases} 100\% & \text{for } N_{00}, \\ 91\% & \text{for } N_{02}. \end{cases} \quad (7.5)$$

Separating the asymmetry A_a into three independent parts as

$$A_a = R(Y_1)A_a^{Y_1} + R(Y_2)A_a^{Y_2} + R(Y_4)A_a^{Y_4}, \quad (7.6)$$

and considering each form factor separately, we obtain the 1 - σ allowed upper bounds of the form factors ($i=1,2,4$)

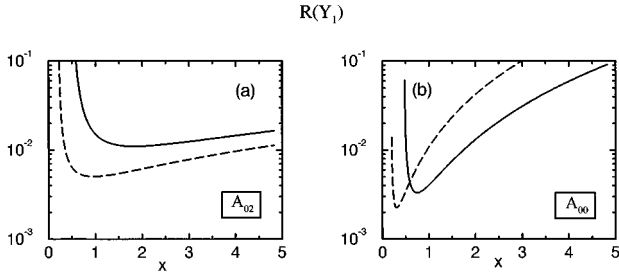


FIG. 4. The x dependence of the $R(Y_1)$ upper bound, $\text{Max}(|R(Y_1)|)$, at $\sqrt{s}=0.5$ and 1.0 TeV, from (a) the asymmetry A_{02} and (b) the asymmetry A_{00} , respectively. The solid lines are for $\sqrt{s}=0.5$ TeV and the long-dashed lines for $\sqrt{s}=1.0$ TeV.

$$\text{Max}(|R(Y_i)|_a) = \frac{\sqrt{2}}{|A_a^{Y_i} \sqrt{\epsilon N_{\text{unpol}}|}}, \quad (7.7)$$

if no asymmetry is found. The N_{SD} - σ upper bound is determined simply by multiplying $\text{Max}(|R(Y_i)|_a)$ and $\text{Max}(|I(Y_4)|_a)$ by N_{SD} .

B. The γWW and $\gamma\gamma WW$ vertices: Y_1 and Y_2

The parity-violating form factors Y_1 and Y_2 respect charge conjugation invariance and they are related to the W electric dipole moment (EDM) d_W and the W magnetic quadrupole moment (MQD) \tilde{Q}_W of W^+ by

$$d_W = \frac{2e}{m_W}(Y_1 + 6Y_2), \quad \tilde{Q}_W = -\frac{4e}{m_W^2}(Y_1 - 6Y_2). \quad (7.8)$$

There are strong indirect phenomenological constraints on the above couplings arising from the EDM of the electron and neutron [21]. However, we should note that there is a possibility of cancellation among different contributions which renders these indirect constraints ineffective. Direct studies of W -pair production at high energies are quite complementary to the precision experiments at low energies. Although the interplay between high- and low-energy experimental constraints is important, the latter constraints cannot replace the role of high-energy experiments.

Figures 4(a) and 4(b) show the x dependence of the sensitivities to $R(Y_1)$, which are obtained from A_{02} and A_{00} ,

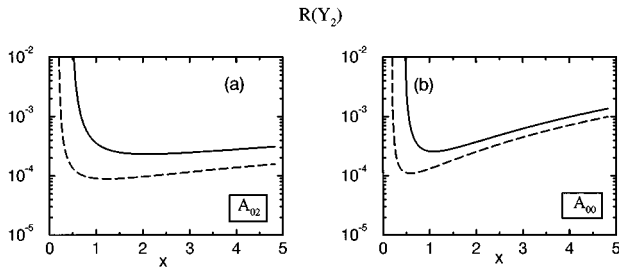


FIG. 5. The x dependence of the $R(Y_2)$ upper bound, $\text{Max}(|R(Y_2)|)$ at $\sqrt{s}=0.5$ and 1.0 TeV, from (a) the asymmetry A_{02} and (b) the asymmetry A_{00} , respectively. The solid lines are for $\sqrt{s}=0.5$ TeV and the long-dashed lines for $\sqrt{s}=1.0$ TeV.

TABLE IV. The best 1 - σ bounds of the CP -odd form factors $R(Y_1)$ and $R(Y_2)$ and their corresponding x values for $\sqrt{s}=0.5$ and 1 TeV.

	A_{02}		A_{00}	
\sqrt{s} (TeV)	0.5	1.0	0.5	1.0
x	1.83	0.96	0.75	0.31
$\text{Max}(R(Y_1))$	1.1×10^{-2}	5.0×10^{-3}	3.2×10^{-3}	2.2×10^{-3}
x	2.09	1.23	1.11	0.59
$\text{Max}(R(Y_2))$	2.4×10^{-4}	9.0×10^{-5}	2.6×10^{-4}	1.1×10^{-4}

respectively, for $\sqrt{s}=0.5$ TeV and $\sqrt{s}=1$ TeV. The x dependence of the sensitivities to $R(Y_2)$ are shown in Figs. 5(a) and 5(b). In both figures, the solid lines are for $\sqrt{s}=0.5$ TeV and the long-dashed lines for $\sqrt{s}=1.0$ TeV. Let us make a few comments on the results shown in the two figures (Figs. 4 and 5) and Table IV.

(i) The sensitivities, especially from the asymmetry A_{00} mode, depend strongly on the value of x . Smaller x values are favored for A_{00} , while relatively large x values are favored for A_{02} . This property can be understood clearly by noting that \hat{A}_{00} gets suppressed as the $\gamma\gamma$ c.m. energy increases, while \hat{A}_{02} does not.

(ii) The optimal sensitivities on $R(Y_2)$ are very much improved as the e^+e^- c.m. energy increases from 0.5 TeV to 1 TeV while those of $R(Y_1)$ are a little improved. The optimal x values are reduced as the c.m. energy increases.

(iii) At the two \sqrt{s} values, the asymmetries $A_{00}^{Y_1}$ give stronger sensitivities than $A_{02}^{Y_1}$ to $R(Y_1)$, while the two symmetries $A_{02}^{Y_2}$ and $A_{00}^{Y_2}$ give rather similar sensitivities to $R(Y_2)$. These properties can be understood from the \hat{s} dependence of the corresponding CP -odd distributions (6.6).

The above results underlie the importance of having adjustable laser frequencies, which allows us to select the regime where each contribution becomes dominant. We find that the two-photon mode allows us to reach the limit that $R(Y_1)$ is of the order of 10^{-3} and $R(Y_2)$ is of the order of 10^{-4} or less.

C. The $\gamma\gamma H$ vertex: Y_4

The $\gamma\gamma H$ vertex Y_4 can be studied in the process $\gamma\gamma \rightarrow H$ [5], where the interference between the one-loop SM amplitudes and the new CP -odd amplitudes lead to observable CP -odd asymmetries. In this paper, we study the sensitivity of the process $\gamma\gamma \rightarrow W^+W^-$ to the CP -odd $\gamma\gamma H$ coupling Y_4 , where m_H is below the W -pair threshold. For an

TABLE V. The 1 - σ sensitivities to the CP -odd form factor $R(Y_4)$ and their corresponding x values for $\sqrt{s}=0.5$ and 1 TeV. Here, $m_H=100$ GeV.

	A_{02}		A_{00}	
\sqrt{s} (TeV)	0.5	1.0	0.5	1.0
x	1.43	0.69	0.76	0.31
$\text{Max}(R(Y_4))$	1.1×10^{-2}	6.4×10^{-3}	7.5×10^{-3}	5.0×10^{-3}

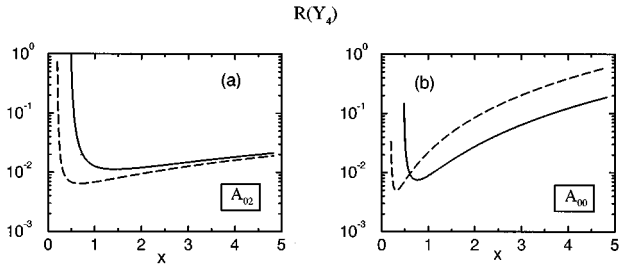


FIG. 6. The x dependence of the $R(Y_4)$ upper bound, $\text{Max}(|R(Y_4)|)$ at $\sqrt{s}=0.5$ and 1.0 TeV, from (a) the asymmetry A_{02} and (b) the asymmetry A_{00} , respectively. Here, the Higgs mass is $m_H=100$ GeV. The solid lines are for $\sqrt{s}=0.5$ TeV and the long-dashed lines for $\sqrt{s}=1.0$ TeV.

actual numerical analysis, we set $m_H=100$ GeV and assume that its width is negligible. Our results are insensitive to m_H as long as $m_H < 2m_W$.

The best sensitivities to $R(Y_4)$ from the asymmetries A_{02} and A_{00} and their corresponding x values for $\sqrt{s}=0.5$ and 1.0 TeV are listed in Table V. Two asymmetries give the approximately same sensitivities at the same x value. The doubling of the e^+e^- c.m. energy improves the sensitivity so much and renders the optimal x values smaller than those at $\sqrt{s}=0.5$ TeV. Figure 6 shows the very strong x dependence of the $R(Y_4)$ $1-\sigma$ sensitivities. Quantitatively, we find that the constraints on $R(Y_4)$ are of the order of 10^{-3} for $m_H=100$ GeV at $\sqrt{s}=0.5$ and 1.0 TeV.

D. Model expectations

In order to assess the usefulness of the two-photon mode with polarized photons, it is useful to estimate the expected size of the CP -odd form factors in a few specific models with reasonable physics assumptions. Several works [2] have estimated the size of the W EDM in various models beyond the SM. They have shown that the W EDM can be of the order 10^{-20} (e cm) in the multi-Higgs-doublet model and the supersymmetric SM, corresponding to Y_1 and Y_2 of the order of 10^{-4} . It is predicted of about 10^{-22} and less than 10^{-38} (e cm) in the left-right model and the SM, respectively,

In more general, if these vertices appear in the one-loop level [22] the coefficients f_i may contain a factor of $1/16\pi^2$. By setting all f_i 's to be $1/16\pi^2$ and setting $\Lambda=v=246$ GeV, we find

$$|Y_1| \sim |Y_3| \sim |Y_4| \sim 10^{-3}, \quad |Y_2| \sim 10^{-4}. \quad (7.9)$$

The above order of magnitude estimates (7.9) of the form factors are consistent with the values expected in some specific models.

It is worth remarking that the two-photon experiments may allow us to probe the CP -odd effects of the expected size (7.9). The two-photon collider with polarized photons and adjustable laser frequency can play a crucial role in probing CP violation in the bosonic sector.

E. Comparison of the $\gamma\gamma$ mode and the e^+e^- mode

The initial e^+e^- state of the $e^+e^- \rightarrow W^+W^-$ process is (almost) CP -even due to the very small electron mass. It is then clear that the initial electron beam polarizations are not so useful to construct large CP -odd asymmetries. CP -violating W interactions can be probed only via spin/angular correlations of the decaying W 's. For $L_{ee}=20 \text{ fb}^{-1}$ and $\kappa=1$, we compare the constraints from the two-photon mode with those from the e^+e^- mode by studying the W^\pm decay correlations at $\sqrt{s}=0.5$ TeV.

The process $e^+e^- \rightarrow W^+W^-$ [12,14] has been investigated in detail. For the present comparison, let us refer to the work by Kalyniak, *et al.* [14], where they have assumed $L_{ee}=50 \text{ fb}^{-1}$ and a perfect detector. Readjusting the e^+e^- integrated luminosity to 20 fb^{-1} , we can summarize their findings; the total cross section with the pure leptonic decay modes of the W 's gives the constraint $|R(Y_1)| \leq 5 \times 10^{-2}$. It is clear from Table IV that the two-photon mode is much more promising than the e^+e^- mode in probing CP violation in the W pair production, if $\kappa \sim 1$ $e\gamma$ conversion rate is technically achieved.

VIII. SUMMARY AND CONCLUSIONS

In this paper we have made a systematic study of observable asymmetries related with two polarized-photon collisions via the Compton backscattered laser beam at future linear colliders, which could serve as tests of possible CP -violating effects. We have described in a general framework how photon polarization is employed to study CP invariance in the initial two-photon state. We have considered the most general dimension-six CP -odd operators in the scalar and vector boson sector, preserving all the SM gauge symmetries in the linear realization of the electroweak symmetry breaking.

Limiting ourselves to purely linearly polarized photon beams, we have constructed two CP -odd asymmetries in the process $\gamma\gamma \rightarrow W^+W^-$. The CP -odd asymmetries can be extracted by simply adjusting the angle between the polarization vectors of two laser beams. We have found that the sensitivities of the CP -odd asymmetries to the CP -odd form factors depend strongly on the e^+e^- c.m. energy and the laser beam frequency.

In Tables IV and V the maximal sensitivities of the CP -odd form factors and the corresponding x values have been shown for $\sqrt{s}=0.5$ and 1 TeV with $\kappa^2 L_{ee}=20 \text{ fb}^{-1}$. The sensitivities are high enough to probe CP -odd new interactions beyond the limits from some specific models with reasonable physics assumptions.

We have found that, for $\kappa \sim 1$, a counting experiment in the two-photon mode with adjustable laser frequency can give much stronger constraints on the W EDM and magnetic quadratic moment (MQD) than the e^+e^- mode can do through the W^\pm decay correlations in e^+e^- collisions using a perfect detector.

To conclude, (linearly) polarized photons by backscattered laser beams of adjustable frequencies at a TeV scale e^+e^- linear e^+e^- collider provide us with a very efficient mechanism to probe CP violation in two-photon collisions.

ACKNOWLEDGMENTS

The authors would like to thank F. Boudjema, F. Cuyper, I. F. Ginzburg, H. S. Song, R. Szalapski, T. Takahashi, C. P. Yuan, and P. M. Zerwas for useful suggestions and helpful comments. The work of S.Y.C. was supported in part by the

Japan Society for the Promotion of Science (No. P-94024) and that of K.H. by the Grant-in-Aid for Scientific Research from the Japanese Ministry of Education, Science and Culture (No. 05228104). The work of M.S.B. was supported by Center for Theoretical Physics, Seoul National University.

-
- [1] M. Kobayashi and T. Maskawa, *Prog. Theor. Phys.* **49**, 379 (1973).
- [2] D. Chang, W.Y. Keung, and J. Liu, *Nucl. Phys.* **B355**, 295 (1991); R. Lopéz-Mobilia and T.H. West, *Phys. Rev. D* **51**, 6495 (1995).
- [3] *Proceedings of the First International Workshop on Physics and Experiments with Linear e^+e^- Colliders*, Saariselka, Finland, 1991, edited by R. Orava, P. Eerola, and M. Nordberg (World Scientific, Singapore, 1992); *Proceedings of the Second International Workshop on Physics and Experiments with Linear e^+e^- Colliders*, Waikoloa, Hawaii, 1993, edited by F.A. Harris, S.L. Olsen, S. Pakvasa, and X. Tata (World Scientific, Singapore, 1993).
- [4] S.Y. Choi and F. Schrempp, *Phys. Lett. B* **272**, 149 (1991); E. Yehudai, *Phys. Rev. D* **44**, 3434, (1991); F. Boudjema and G. Bélanger, *Phys. Lett. B* **288**, 2288 (1992); *Proceedings of the Workshop on Gamma-Gamma Colliders*, LBL, Berkeley, California, 1994, edited by S. Chattopadhyay and A.M. Sessler [*Nucl. Instrum. Methods Phys. Res. A* **355**, 1 (1995)]; M. Bailargeon, G. Bélanger, and F. Boudjema, in *Proceedings of Two-Photon Physics from DAΦNE to LEP200 and Beyond*, Paris, 1994 (World Scientific, Singapore, 1994).
- [5] J.F. Gunion and H.E. Haber, *Phys. Rev. D* **48**, 5109 (1993); P.M. Zerwas, in *Proceedings of the Eighth International Workshop on Photon-Photon Collisions*, Shores (Jerusalem Hills), 1988 (World Scientific, Singapore, 1988); S.J. Brodsky, in *Proceedings of the Workshop on Physics and Experiments with Linear e^+e^- Colliders*, Ref. [3]; J.F. Gunion, *ibid.*; D.L. Borden, D.A. Bauer, and D.O. Caldwell, Report No. SLAC-PUB-5715 (unpublished); *Phys. Rev. D* **48**, 4018 (1993).
- [6] B. Grażadkowski and J.F. Gunion, *Phys. Lett. B* **291**, 361 (1992); M. Krämer, J. Kühn, M.L. Stong, and P.M. Zerwas, *Z. Phys. C* **64**, 21 (1994); J.F. Gunion and J.G. Kelly, *Phys. Lett. B* **333**, 110 (1994).
- [7] W. Bernreuther and A. Brandenburg, *Phys. Lett. B* **314**, 104 (1993); W. Bernreuther, J.P. Ma, and B.H.J. McKellar, *Phys. Rev. D* **51**, 2475 (1995); H. Anlauf, W. Bernreuther, and A. Brandenburg, *ibid.* **52**, 3803 (1995); **53**, 1725(E) (1996).
- [8] J.P. Ma and B.H.J. McKellar, *Phys. Lett. B* **319**, 533 (1993).
- [9] G. Bélanger and G. Couture, *Phys. Rev. D* **49**, 5720 (1994).
- [10] S.Y. Choi and K. Hagiwara, *Phys. Lett. B* **359**, 369 (1995).
- [11] K. Hikasa, *Phys. Lett.* **143B**, 266 (1984); *Phys. Rev. D* **33**, 3203 (1986).
- [12] K. Hagiwara, R.D. Peccei, D. Zeppenfeld, and K. Hikasa, *Nucl. Phys.* **B282**, 253 (1987).
- [13] G. Gounaris, D. Schildknecht, and F.M. Renard, *Phys. Lett. B* **263**, 291 (1991); M.B. Gavela, F. Iddir, A. Le Yaouanc, L. Oliver, O. Péne, and J.C. Raynal, *Phys. Rev. D* **39**, 1870 (1989); A. Bilal, E. Massó, and A. De Rújula, *Nucl. Phys.* **B355**, 549 (1991); G. Gounaris, J.L. Kneur, J. Layssac, G. Moultaqa, F.M. Renard, and D. Schildknecht, in *e^+e^- Collisions at 500 GeV: The Physics Potential*, Proceedings of the Workshop, Munich, Annecy, Hamburg, 1991, edited by P.M. Zerwas (DESY Report No. 93-123C, Hamburg, 1993), p. 735.
- [14] P. Kalyniak, P. Madsen, N. Sinha, and R. Sinha, *Phys. Rev. D* **52**, 3826 (1995).
- [15] I.F. Ginzburg, G.L. Kotkin, V.G. Serbo, S.L. Panfil, and V.I. Telnov, *Zh. Éksp. Teor. Fiz. Pis'ma Red.* **34**, 514 (1981) [*JETP Lett.* **34**, 491 (1982)]; *Nucl. Instrum. Methods* **205**, 47 (1983); I.F. Ginzburg, G.L. Kotkin, S.L. Panfil, V.G. Serbo, and V.I. Telnov, *ibid.* **219**, 5 (1984); V.I. Telnov, *ibid.* **A294**, 72 (1992); Proceedings of the First Workshop on Physics and Experiments with Linear e^+e^- Colliders Saariselka, Finland, 1991, edited by R. Orava, P. Eerola, and M. Nordberg (World Scientific, Singapore, 1992); D. L. Borden, in *Proceedings of the Second International Workshop on Physics and Experiments with Linear e^+e^- Colliders*, Ref. [3],
- [16] K. Hagiwara and M. Stong, *Z. Phys. C* **62**, 99 (1994).
- [17] V.B. Berestetskii, E.M. Lifshitz, and L.P. Pitaevskii, *Relativistic Quantum Theory* (Pergamon, Oxford, 1971), Pt. I, Chap. 1.
- [18] The authors in Ref. [9] also has considered the distribution $\mathcal{I}(\Sigma_{02})$, but not the distribution $\mathcal{I}(A_{00})$.
- [19] The function $A_{\eta\eta}$ has been considered by Krämer *et al.* [6].
- [20] Particle Data Group, L. Montanet *et al.*, *Phys. Rev. D* **50**, 1173 (1994).
- [21] W. Marciano and A. Queijeiro, *Phys. Rev. D* **33**, 3449 (1986); F. Boudjema, K. Hagiwara, C. Hamzaoui, and K. Numata, *ibid.* **43**, 2223 (1991); A. De Rújula, M. Gavela, O. Péne, and F. Vegas, *Nucl. Phys.* **B357**, 311 (1991); see also S. Barr and W. Marciano, *CP Violation*, edited by C. Jarlskog (World Scientific, Singapore, 1989).
- [22] C. Arzt, M.B. Einhorn, and J. Wudka, *Nucl. Phys.* **B433**, 41 (1995), and references therein.